Since January 2020 Elsevier has created a COVID-19 resource centre with free information in English and Mandarin on the novel coronavirus COVID-19. The COVID-19 resource centre is hosted on Elsevier Connect, the company's public news and information website.

Building and Environment 227 (2023) 109804

Contents lists available at ScienceDirect

Building and Environment

journal homepage: www.elsevier.com/locate/buildenv

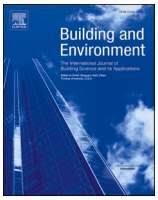

Large-scale evaluation of microorganism inactivation by bipolar ionization and photocatalytic devices

Katherine M. Ratliff [a,*], Lukas Oudejans [a], John Archer [a], Worth Calfee [a], Jerome U. Gilberry [b], David Adam Hook [b], William E. Schoppman [b], Robert W. Yaga [b], Lance Brooks [a], Shawn Ryan [a]

[a] Center for Environmental Solutions and Emergency Response, Office of Research and Development, U.S. Environmental Protection Agency, Research Triangle Park, NC, USA

[b] Jacobs Technology Inc., Research Triangle Park, NC, USA

ARTICLE INFO

Keywords:
Bipolar ionization
Photocatalytic oxidation
Bacteriophage MS2
Pesticide device
Indoor air cleaning
Air treatment

ABSTRACT

The COVID-19 pandemic has raised awareness in the spread of disease via airborne transmission. As a result, there has been increasing interest in technologies that claim to reduce concentrations of airborne pathogens in indoor environments. The efficacy of many of these emerging technologies is not fully understood, and the testing that has been done is often conducted at a small scale and not representative of applied settings. There is currently no standard test method for evaluating air treatment technologies, making it difficult to compare results across studies or technology types. Here, a consistent testing approach in an operational-scale test chamber with a mock recirculating heating, ventilation, and air conditioning (HVAC) system was used to evaluate the efficacy of bipolar ionization and photocatalytic devices against the non-enveloped bacteriophage MS2 in the air and on surfaces. Statistically significant differences between replicate sets of technology tests and control tests (without technologies active) are apparent after 1 h, ranging to a maximum of 0.88 $\log_{10}$ reduction for the bipolar ionization tests and 1.8 $\log_{10}$ reduction for the photocatalytic device tests. It should be noted that ozone concentrations were elevated above background concentrations in the test chamber during the photocatalytic device testing. No significant differences were observed between control and technology tests in terms of the amount of MS2 deposited or inactivated on surfaces during testing. A standardized, large-scale testing approach, with replicate testing and time-matched control conditions, is necessary for contextualizing laboratory efficacy results, translating them to real-world conditions, and for facilitating technology comparisons.

1. Introduction

The coronavirus disease 2019 (COVID-19) pandemic has raised awareness about the role of airborne pathogens in the spread of disease [1–8]. As an infected person sheds aerosol particles and droplets, others can come in contact with those pathogens, either in the air or on surfaces [4]. There are now many documented cases of COVID-19 outbreaks that have occurred in shared indoor spaces [4,9–11]. In addition to COVID-19, there is evidence that many other respiratory viruses, including influenza, respiratory syncytial virus (RSV), human rhinovirus, and Middle East respiratory syndrome (MERS)-CoV, are spread primarily through airborne transmission [8]. As such, there has been increasing interest in utilizing *in situ* technologies that are designed to reduce the concentration of airborne pathogens, either through particle trapping and removal or microorganism inactivation. These technologies could be particularly beneficial in locations where it is difficult to improve ventilation [12] and can be either installed as part of heating, ventilation, and air conditioning (HVAC) systems (or other fixed locations within rooms) or deployed as in-room portable units. The growing interest in these air treatment technologies, which include traditional mechanical filtration, ultraviolet-C (UV-C) irradiation (including Far-UVC [13]), chemical treatment, photocatalytic oxidation, and ionizers [14], has increased the rate at which they are marketed and utilized for this purpose.

Two particular categories of these technologies – bipolar ionization and photocatalytic oxidation – have garnered increasing attention in recent years as a result of the COVID-19 pandemic. Bipolar ionization devices, which have become more widely installed in a range of settings (e.g., schools, churches, and hospitals), generate both positive and negative ions that can react with airborne contaminants. They have been

* Corresponding author. 109 TW Alexander Drive, Research Triangle Park, NC, 27711, USA.
E-mail address: Ratliff.Katherine@epa.gov (K.M. Ratliff).

https://doi.org/10.1016/j.buildenv.2022.109804
Received 18 August 2022; Received in revised form 20 October 2022; Accepted 8 November 2022
Available online 12 November 2022
0360-1323/Published by Elsevier Ltd.

proposed for use to reduce concentrations of particulate matter, volatile organic compounds, and pathogens in the air [15,16]. The air ionization process generates reactive species that have been observed to inactivate viruses and bacteria in the air and on surfaces [17–21], increase the particle trapping efficiency of various filter media [22–24], and increase particle deposition rates [25]. Photocatalytic oxidation, which combines the use of photocatalytic materials (e.g., titanium dioxide [26]) and ultraviolet (UV) light, is another technology that has been proposed for use to reduce the risk of disease transmission; airborne microorganisms can be directly inactivated by the UV light or by the oxidative radicals generated through irradiating a photocatalytic surface. In addition to removing contaminants from the air, photocatalytic processes have also been used for water treatment [27,28]. Effectiveness of photocatalytic oxidation against pathogens is a function of the UV wavelength and dose (i.e., the product of UV irradiation time and light intensity), as well as the photocatalyst composition [29,30].

There is limited information to evaluate how effective these emerging air treatment technologies are against airborne viruses and other pathogens relative to more established methods, such as mechanical filtration. Although both bipolar ionization and photocatalytic devices are regulated by the U.S. Environmental Protection Agency (EPA) under the Federal Insecticide, Fungicide, and Rodenticide Act (FIFRA) in that false or misleading claims cannot be made about device efficacy or safety (in addition to some administrative requirements), the vendor's performance claims are not routinely reviewed or verified by the EPA as part of a registration process, as is done for pesticide products [31]. Because there is currently no established standardized test method to assess the efficacy of air treatment technologies (although the Association of Home Appliance Manufacturers [AHAM] did recently release AHAM AC-5-2022, "Method for Assessing the Reduction Rate of Key Bioaerosols by Portable Air Cleaners Using an Aerobiology Test Chamber", specific to portable household air cleaners) [32], comparing methodologies and results across different studies and technology types is difficult. What testing has been conducted is often done in a small-scale laboratory setting under conditions that are designed to maximize device performance (as commissioned by the device manufacturers), leading to results that are not easily extrapolated to applied settings (e.g., artificially high air exchange rates). In addition, some of these air cleaning technologies may emit harmful byproducts when operated (e.g., ozone, carbon monoxide, formaldehyde) or when their emissions interact with other materials and surfaces in indoor environments, raising concerns about their safety [15,33].

The objective of this study was to use a large-scale test chamber and standardized testing approach to evaluate the effectiveness of bipolar ionization and photocatalytic devices in reducing virus concentrations in the air and on surfaces. The devices tested were selected with input from research stakeholders (including EPA regulatory offices and large transit agencies) and installed in a recirculating HVAC system that was constructed in an aerosol test chamber for this study. Conducting research with aerosolized microorganisms at large scales necessitates the use of safer, e.g., Biosafety Level (BSL)-1 surrogate organisms instead of using pathogenic agents, such as SARS-CoV-2 (BSL-3). Accordingly, the bacteriophage MS2, a non-enveloped virus that infects *Escherichia coli*, was used for this work. An additional advantage of using MS2 is that, as a non-enveloped virus, it is expected to be more resistant to chemical inactivation than enveloped viruses (such as SARS-CoV-2) [34], meaning that the efficacy results reported here are potentially relevant to a wider range of pathogens. Performing these efficacy tests at a large scale and with recirculating air flow, which is more representative of conditions that would be found in a range of indoor settings (compared to static, small-scale chamber tests) [35,36], is informative for translating research findings to scenarios where these devices could be deployed. (Of note is that 100% of the chamber air is recirculated with no fresh air introduction during testing, representing a more conservative test condition.) Developing and evaluating standardized testing protocols for testing air treatment devices facilitates cross-study and cross-technology comparisons.

2. Materials and methods

Experiments were conducted in a large-scale test chamber with a constructed recirculating mock HVAC system to evaluate how effectively bipolar ionization and photocatalytic devices inactivate MS2 in the air and on surfaces. An objective of the study design was to maintain a high enough concentration of viable aerosolized MS2 throughout the duration of testing in control conditions (without the technologies active) to be able to demonstrate a 3-$\log_{10}$ reduction in airborne virus concentration during test conditions (with technologies active) relative to the time-matched control tests. A 3-$\log_{10}$ reduction is the performance benchmark for pesticide product virucidal claims [31] and for air sanitizer claims [37].

2.1. Test chamber

A 12 ft × 10 ft x 25 ft (3000 ft^3) section of a recirculating aerosol wind tunnel at EPA's Aerosol Test Facility in Research Triangle Park, NC was sectioned off and used as the test chamber for this research (Fig. 1, Fig. S1). The chamber consists of a painted steel frame with a painted plywood and sheet metal flooring, glass panels on the long sides, and 4-mil plastic sheeting on short sides (Item #730809, Project Source [a Lowe's Brand], Mooresville, NC, USA) with ZipWall, LLC (Arlington, MA, USA) supports and zippers to provide access and allow for airflow through the chamber between tests. The facility is equipped with a supervisory control and data acquisition (SCADA) system that is used to regulate environmental conditions that are set prior to testing. Temperature is controlled using a cooling coil chilled water system, and relative humidity (RH) is controlled using a desiccant dehumidifier and a deionized water steam humidifier. The wind tunnel is outfitted with multiple high-efficiency particulate air filter (MERV16) banks, which are used to filter the chamber air before and after testing. All experiments were conducted at 22 ± 2 °C and a RH of 30–35%. This RH was selected because virus viability is reduced at a higher RH (lowest at ~50%) [38], and an objective of the study design was to create a relatively high bioaerosol challenge concentration for the air cleaning technologies.

A mock HVAC system was designed and constructed in the test chamber from galvanized steel duct materials to represent a range of indoor and transit vehicle settings (Fig. 1, Fig. S1). An Omni-Aire 1000V (Omnitech, Mukilteo, WA) negative air machine (NAM), with the HEPA filter removed, represents a cold air return, recirculating air through the HVAC system and test chamber (with no filter present in the HVAC system for any of these experiments). During testing, 100% of the air is recirculated, and no fresh air is introduced. A rectangular section downstream of the air return with a 14-inch x 14-inch cross section serves as the installation section for the devices evaluated in this research (Fig. 1, Fig. S1C). Air passing by the installed devices flows through an 8-inch main duct before being directed through six evenly spaced 6-inch branches. These branches distribute air back into the chamber through 10-inch round supply diffusers with butterfly dampers at evenly spaced distribution points located throughout the chamber near the ceiling (approximately 7.5 ft above the chamber floor). For the tests conducted here, the NAM airflow rate is set to 350 cubic feet per minute (CFM), resulting in approximately 7 air changes per hour (ACH) in the chamber.

Two metal fans (LASKO 2265 QM, West Chester, PA) placed in opposite corners of the chamber (Fig. 1A), behind where the bioaerosol is introduced, operate during testing at 1448 ft/min to facilitate mixing in the chamber. In between tests, the chamber air is reset by opening the plastic sheeting on the short ends of the chamber and flushing HEPA-filtered air through the chamber until negligible particle counts are detected in the chamber. Replicate bioaerosol samples taken from different locations within the test chamber were consistent at each

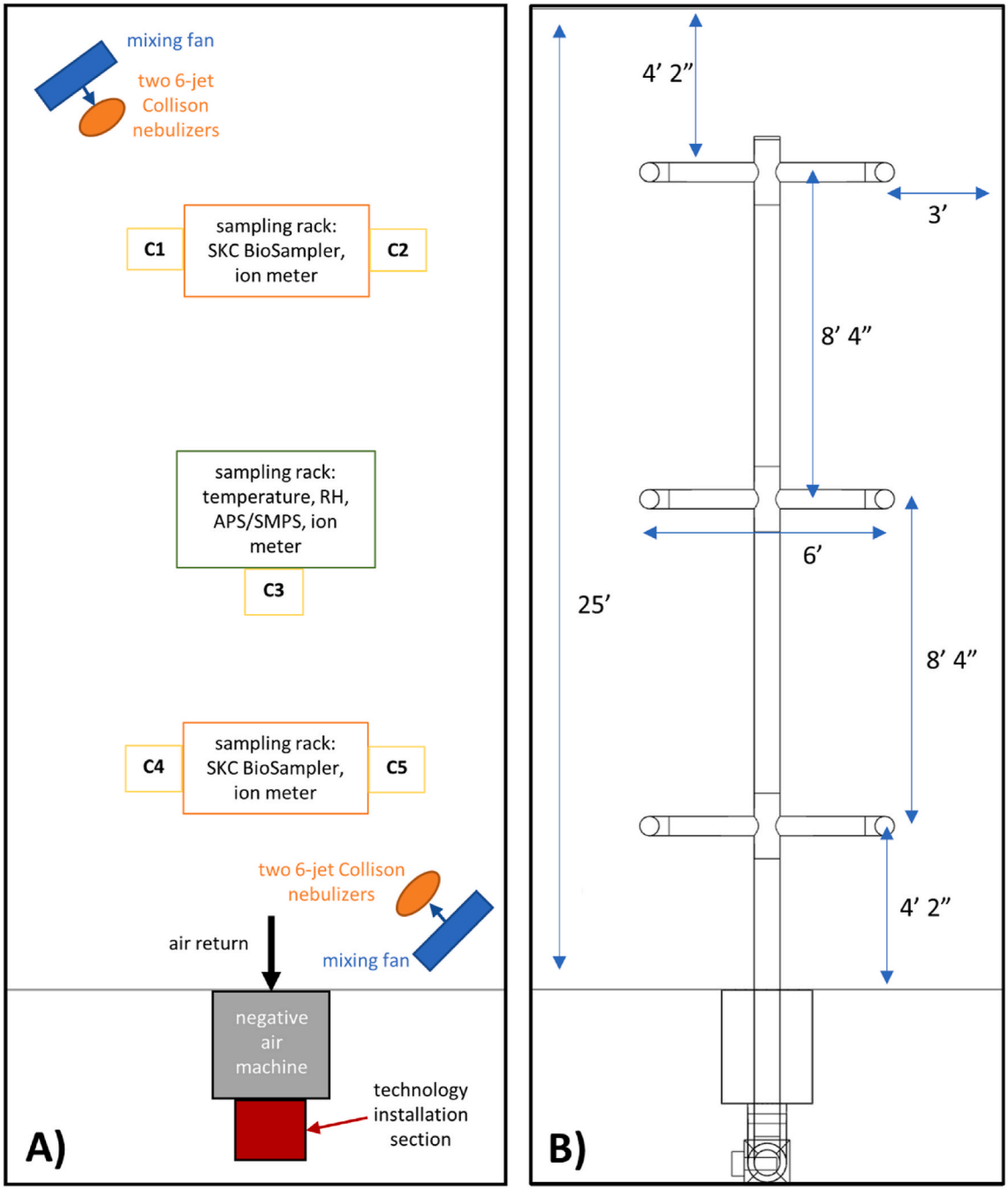

Fig. 1. Top-down view of test chamber layout with A) locations of testing equipment and sampling locations labeled, where C1 – C5 denote (when included during a test) where the deposition and inoculation coupons were placed, side by side, on the chamber floor, and B) mock HVAC ductwork schematic and relevant dimensions labeled. Not drawn to scale.

sampling time point throughout testing, suggesting that the test chamber air is well mixed.

2.2. Microbiological methods

The bacteriophage MS2 (ATTC 15597-B1), a non-enveloped virus that infects *Escherichia coli* (ATCC 15597), was used in this study. MS2 is expected to be more resistant to chemical inactivation than enveloped viruses (e.g., SARS-CoV-2) [34,39] and, as a BSL-1 microorganism, poses fewer biosafety concerns for large-scale bioaerosol studies.

2.2.1. MS2 phage propagation

Working stocks of MS2 were prepared using a top agar overlay technique [40], where solid agar plates made with lysogeny broth (LB) agar (BD Difco 240110, Thermo Fisher Scientific, Waltham, MA) were coated with ~6 mL of molten LB top agar containing 100 μL of MS2 stock and 100 μL of a log-phase *E. coli* C-3000 bacterial culture (OD_{600} ~0.5–0.7) and incubated overnight 35 ± 2 °C. Following incubation, a sterile cell spreader was used to scrape the soft agar overlay from three 100 mm plates into a sterile 50-mL conical tube containing 15 mL of SM buffer (S0249, Teknova Inc., Hollister, CA), vortexed (Vortex Genie 2, part no. 3030A, Daigger Scientific, Inc., Vernon Hills, IL) for approximately 2 min to break up agar clumps, and then centrifuged (Heraes Megafuge 16R, Thermo Fisher Scientific, Waltham, MA) for 15 min at 7000×*g*. The supernatant was then slowly removed from each tube and filtered using a 0.2 μm syringe filter (PES syringe filters, 431229,

Corning Inc., Corning, NY, USA). The filter-sterilized MS2 stocks in SM buffer were stored in cryovials at −80 °C until use.

2.2.2. MS2 aerosolization

Four 6-Jet Collison Nebulizers (part no. ARGCNB3, CH Technologies, Westwood, NJ) were used to aerosolize MS2 during each experiment, with two pairs of nebulizers operating in opposite corners of the chamber in front of the mixing fans (Fig. 1A). A 10 mL mixture of 1:4 parts MS2 stock (thawed at room temperature and vortexed until no crystals remain) to 0.22 μm filter-sterilized deionized water with 6 drops of Antifoam A (Sigma-Aldrich, St. Louis, MO) was added to each nebulizer. An inoculum concentration check was performed for each test by enumerating both the inoculum before it was divided into the nebulizers and the inoculum from each nebulizer. Each nebulizer was outfitted with a polycarbonate precious fluids jar (part no. ARGJAR0002, CH Technologies, Westwood, NJ) and a precious fluids extension sleeve. (part no. ARGCNB0038, CH Technologies, Westwood, NJ). MS2 was aerosolized over a 10-min period using dried compressed air at 40 psi with a flow rate of 20 L per minute and approximately 0.28 mL of fluid distributed per minute at each nebulizer.

2.2.3. Bioaerosol sampling

Air from the test chamber was sampled using two SKC BioSamplers (SKC Inc., Eighty-Four, PA) connected to air sampling pumps operating at a rate of 12.5 L/min each. Each sampling period for the tests described herein was 10 min, resulting in a total air volume of 125 L of air drawn during each sampling period per sampler. Sample times in figures and in the text below note the start of the 10-min sample period. The samples were collected at "breathing zone" height (~5 ft above the floor) using 1/4-inch conductive silicone rubber tubing (Simolex, Plymouth, MI) to draw air from the sampling location to the BioSamplers, which were located outside of the test chamber to facilitate changing samplers during testing. The first air test sample (time = 0 min sample) was collected immediately following the 10-min MS2 aerosolization period. Background samples were also collected prior to MS2 aerosolization to ensure no viable virus was present in the chamber air prior to the start of each test. Each BioSampler contained 20 mL of 1 × phosphate-buffered saline (PBS) (P0196, Teknova, Hollister, CA, USA) as the collection media. The liquid samples were stored on ice (or refrigerated at 4 °C) between collection and plating and were vortexed continuously for 2 min prior to plating. Samples were plated using a conventional soft agar overlay method [41] using various 10-fold dilutions with 100 μL aliquots or undiluted with 100 μL and/or 1 mL aliquots.

2.2.4. MS2 Surface Samples

Deposition of viable MS2 on surfaces and inactivation of MS2 on surfaces was also evaluated using uniform pieces of 2 cm × 4 cm stainless-steel material (coupons). The material coupons were prepared for testing by washing in Liquinox anionic liquid detergent (Alconox, White Plains, NY, USA) according to the manufacturer's instructions, rinsed in deionized water, and dried; they were then soaked in 100% ethanol, rinsed in deionized water, and dried; and finally, they were sterilized by autoclave using a 121 °C gravity cycle (SV 120 scientific pre-vacuum sterilizer; STERIS Amsco, Mentor, OH, USA). Coupons intended to measure the deposition of viable MS2 ("deposition coupons") were placed in the chamber clean, with no virus added prior to testing. Coupons intended to assess the inactivation efficacy of the treatment technologies ("inactivation coupons") were inoculated with thawed MS2 stock prepared in 1 × PBS with 5% Fetal Bovine Serum (FBS, Gibco 10082139, Thermo Fisher Scientific, Waltham, MA, USA). Each inactivation coupon was inoculated with a 10 μL droplet of the prepared inoculum at a target concentration of 10^7 PFU/coupon, which was spread over at least 75% of the surface of the coupon using the pipette tip and dried prior to the test.

Following each test, both the deposition and inactivation coupons were aseptically placed into 50-mL conical tubes containing 10 mL of PBS and extracted by vortexing continuously for 2 min. For each sample, tenfold serial dilutions were prepared in 1 × PBS, and each dilution was plated in triplicate with the bacterial host *E. coli* using a conventional soft overlay method [41]. Plaques were manually enumerated after overnight incubation at 35 ± 2 °C.

For tests where they were included, the deposition and inactivation test coupons were placed side by side on the chamber floor at locations noted in Fig. 1A. For each of these tests where inactivation coupons were included, three positive control coupons were inoculated and extracted according to the procedures outlined above, except they were placed outside the test chamber, so they were not exposed to the technologies (but the handling and duration between inoculation and extraction were the same as the test inactivation coupons). These coupons were placed in the chamber (i.e., instead of in the HVAC ductwork in closer proximity to the technology) to assess the potential impact of these technologies on microorganism loading on surfaces in locations within the chamber, which are more relevant for surfaces that could play a role in contact transmission of some diseases compared to in-duct surfaces.

2.3. Particle measurements

Particle size distribution measurements were also taken throughout each test. To measure particle size diameters between 0.5 μm and 20 μm, an Aerodynamic Particle Sizer (APS, Model 3321, TSI Inc., Shoreview, MN) was used. To measure particle size diameters between 0.01 μm and 0.5 μm, a Scanning Mobility Particle Sizer (SMPS, Model 3080 Electrostatic Classifier/TSI 3010 Condensation Particle Counter, TSI Inc., Shoreview, MN) was used. Air samples for both sets of measurements were collected from the middle of the chamber (Fig. 1A) at the same height as the SKC BioSamplers (5 ft).

2.4. Test devices

A cold plasma bipolar ionization (BPI) device that is sized to treat 2000–4000 ft^2 of living space was installed in the HVAC duct (Fig. 1) and operated continuously during tests where the technology was active. The unit contains a catalytic conversion unit to convert ozone generated by the cold plasma tube to oxygen. The device was operated in the sealed chamber for either 30 or 90 min prior to MS2 aerosolization. Three Air Ion Counter Model AIC2 (AlphaLab, Inc., Salt Lake City, UT) ion meters were located in the test chamber at the height of the bioaerosol sampling ports (5 ft), grounded, and operated in negative polarity mode. Ozone concentration was measured during testing using an Aeroqual Series 500 portable air quality monitor (Aeroqual Limited, Auckland, NZ) outfitted with a 0–0.5 parts per million (ppm) sampling head (detection limit 0.001 ppm).

Two different photocatalytic oxidation (PCO) devices, which use metallic catalysts and Ultraviolet-C (UVC) light to convert water vapor from the air into hydrogen peroxide and other reactive oxides and ions, were used in this study. The device with a smaller catalytic cell (designed to be used with an HVAC blower operating at 250–1200 CFM) will hereafter be referred to as the "PCO1" device, and the device with a larger catalytic cell (designed to operate with an HVAC blower at 1200–3000 CFM) is referred to as the "PCO2" device. For tests conducted with the PCO1 unit, the device was operated for 30 min in the sealed test chamber prior to MS2 aerosolization, and the PCO2 unit was operated for 5 min prior to MS2 aerosolization. Hydrogen peroxide concentration was continuously monitored during testing using a SC-8000 Portable Toxic Gas Monitor (RKI Instruments, Union City, CA, USA) outfitted with a hydrogen peroxide gas sensor with a detection limit of 20 ppb. The same ion meters (with 2 m operating in negative polarity mode and one operating in positive polarity mode) and ozone monitor described above were also continuously operating during the photocatalytic device tests.

Both devices were installed and operated following manufacturer instructions.

2.5. Calculations and statistics

For bioaerosol samples, efficacy (log_{10} reduction) was calculated at each sampling time point as difference between the mean log_{10} concentration of viable MS2 in the air sampled during control tests (where technologies were present in the chamber, but not active) and the sampled concentration during tests with the technologies active. All statistical calculations were performed using Python (version 3.7.3) with the packages NumPy (version 1.16.2), pandas (version 0.24.2), and SciPy (version 1.2.1). For relevant data, a normality check was performed on log_{10}-transformed data using a Shapiro-Wilk test. For data meeting the normality assumption, Welch's t-tests were used to assess differences in group means for paired data, and significance was determined at the $\alpha = 0.05$ level.

3. Results

A total of 16 chamber tests were conducted: five BPI device tests, six photocatalytic device tests (three of each for the PCO1 and PCO2 units), and five controls (with no technology active). All tests were subject to the same environmental conditions (temperature, humidity, airflow), with the only difference being the technology that was installed in the ductwork (Fig. 1), or no technology operating (control tests). All tests were conducted over a span of 90 min (sampling periods beginning at time = 0, 15, 30, 60, and 90 min), except for controls C and D and BPI tests D and E, which were conducted for 120 min (sampling periods beginning at time = 0, 30, 60, 90, and 120 min).

3.1. Bipolar ionization device

The cold plasma bipolar ionization device was powered for 30 min in the sealed chamber prior to the aerosolization of MS2 for tests A and B and for 90 min prior to tests C, D, and E, resulting in an average ion concentration of approximately 1000–2000 counts/cm^3 and 2500–6000 counts/cm^3, respectively, prior to MS2 aerosolization (Fig. S2 for representative ion concentration graphs). The aerosolization process generates charged aerosol particles, contributing to a peak in the resulting ion meter that largely represents the generation of charged particles during MS2 aerosolization (i.e., not ions generated by the bipolar ionization device). Following nebulization, although the ionization device was continuously operating and continuously generating ions, the concentration of ions detected fell to close to background as a result of the interaction between the ions and aerosol particles and potential charge neutralization that results (Fig. S2). Ozone concentration was continuously monitored during testing and was not elevated above background levels, as the device includes a catalytic ozone absorption unit.

The concentration of airborne MS2 over time during each replicate test and control experiment is shown in Fig. 2. The MS2 recoveries (in PFU/m^3) are all normalized to the initial time = 0 min concentration from each respective test such that the variability in recoveries between tests is not impacted by differences in the initial bioaerosol concentration in the chamber. That initial MS2 concentration, with a sampling period starting immediately following aerosolization, was greater than 1×10^8 PFU/m^3 for all test and control experiments (mean initial concentration of 8.5 ± 0.2 log_{10} PFU/m^3). The control experiments demonstrate that natural decay, settling, and wall loss of airborne MS2 alone can lead to a >3 log_{10} reduction in the concentration of bioaerosols in the test chamber over 2 h. The variability among samples collected at the same testing time points during different replicate tests ranges to nearly 1 log_{10} during control experiments (maximum normalized difference of 0.99 log_{10} at 120 min) and slightly greater during tests with the technology active (maximum normalized difference of 1.2 log_{10} at 90 min).

The MS2 concentrations at each sampling time point averaged over the respective control and BPI test sets, as well as the calculated log_{10} reductions at each sampling time point, are shown in Fig. 3. Calculated log_{10} reduction values are also listed in Table 1. During the initial sampling periods (time = 0, 15, 30 min), there were minimal observed differences between the control and BPI test MS2 recoveries, but at time = 60 min (and beyond), the average MS2 recoveries from the tests with the BPI device active were lower than those during the control tests. Following a normality check (Table S1), Welch's *t*-test was used to compare the normalized MS2 recoveries at each sampling time point from the control and BPI tests (Table 1). The only statistically significant (at the $\alpha = 0.05$ level) difference between the MS2 concentrations in the control and BPI tests occurred at the time = 60 min sample point (log_{10}

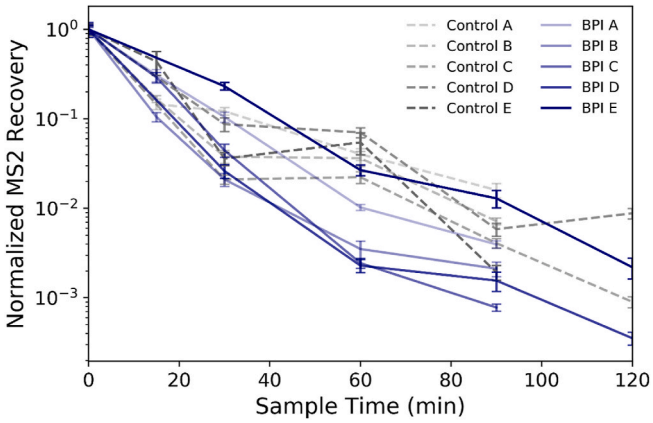

Fig. 2. Normalized MS2 recoveries at each sampling time point throughout the control and bipolar ionization (BPI) tests with the device active. Each time point represents recovery of MS2 from duplicate bioaerosol samples as determined by plaque assay, and the error bars represent pooled standard deviation from triplicate sample plating of duplicate bioaerosol samples for each sampling time point. Data from each sampling time point are normalized to the initial sample recovery at time = 0 min for each individual test.

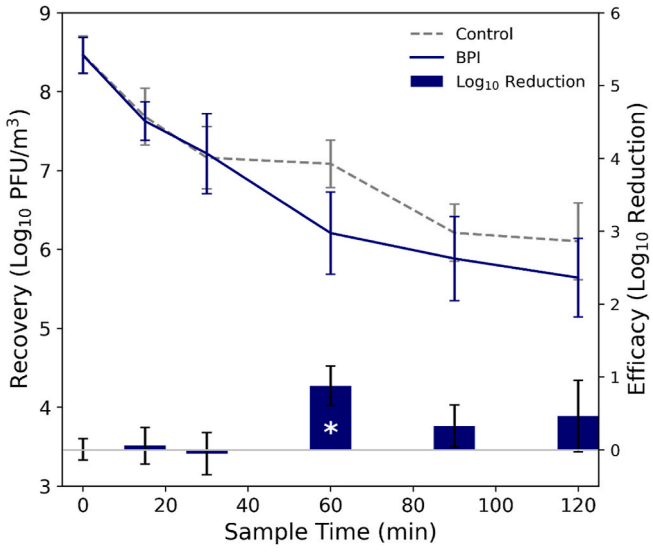

Fig. 3. (Left axis) Concentration of MS2 in the air at each sampling time point during the control and bipolar ionization (BPI) test experiments, averaged over each test set, where error bars represent standard deviation in each set of recoveries. (Right axis) Efficacy of the BPI device against aerosolized MS2, calculated as log_{10} reduction in MS2 recoveries from the control vs. the BPI test experiments; statistical significance between control and technology experiments at the sample times is denoted by (*). For recoveries, error bars represent standard deviation in log_{10} recoveries for each respective set of control and BPI experiments at each sample time; for efficacy, the error bars represent pooled standard error from both the control and technology experiments.

Table 1
Calculated $\log_{10}$ reductions and p-values from paired Welch's *t*-test at each sampling time point comparing recoveries of MS2 from control tests and technology tests. **Bold** text indicates a statistically significant difference ($\alpha < 0.05$) between replicate sets of control recoveries and technology test recoveries.

Technology	Sample Time	Log_{10} Reduction	p-value
BPI	15	0.057	0.94
	30	−0.053	0.81
	60	**0.88**	**0.010**
	90	0.33	0.25
	120	0.46	0.51
PCO1	15	0.095	0.51
	30	0.42	0.69
	60	**1.1**	**0.034**
	90	**0.82**	**0.042**
PCO2	15	0.60	0.19
	30	0.74	0.23
	60	**1.8**	**0.00031**
	90	**1.5**	**0.0010**

reduction = 0.88 [87% reduction], p-value = 0.01). Following the methodology described in Stephens, Gall [42], the clean air delivery rate (CADR), calculated by evaluating the difference in the loss rate constants for MS2 in the experiments with the technology active compared to the control experiment (Fig. S3), multiplied by the chamber volume, is 34 ft^3/min for the BPI device.

The normalized particle concentration in the test chamber over time (where the concentration over time for each respective test is normalized by the maximum particle concentration during each test, typically corresponding to the initial particle count measurement, which was taken directly following the 10-min aerosolization period) is shown in Fig. 4A. In general, the particle concentrations between the control and bipolar ionization device tests appear similar, with a decay in particle concentration over time. The average particle size during both sets of tests also increased as a result of particle agglomeration; Fig. 4B shows the count median diameter (CMD) over time during the course of testing, averaged over each set of control and bipolar ionization tests. Fig. S4 shows an example of the shifting in particle size distribution during testing, with the peak particle size growing larger throughout the tests, and the total particle count decreasing.

3.2. Photocatalytic devices

Concentrations of ozone (Table S2), hydrogen peroxide, and ions were monitored continuously throughout the duration of the photocatalytic device testing. By the end of the test period during the PCO1 tests (the device was also operated 30 min prior to MS2 aerosolization), the ozone concentration was slightly elevated above background concentrations in the chamber (~10 ppb) at an average concentration of 31 ppb at 90 min. The PCO2 unit, which was operated for 5 min prior to MS2 aerosolization, generated greater amounts of ozone, with an average concentration in the chamber of 105 ppb and 131 ppb at 60 and 90 min, respectively. Hydrogen peroxide was not detected throughout the duration of testing with either the PCO1 or PCO2 unit (meter detection limit 20 ppb). Neither unit generated appreciable ion concentrations above counts that were generated in the control tests.

Fig. 5 shows the concentration of airborne MS2 sampled over time during each test and control experiment. For each test, all of the sampled MS2 recoveries (in PFU/m^3) are normalized to the initial time = 0 min sampled concentration for that test. The initial MS2 concentration in all experiments was $>1 \times 10^8$ PFU/m^3 for all experiments, except for the PCO2 experiment C, which had a concentration of MS2 at time = 0 min

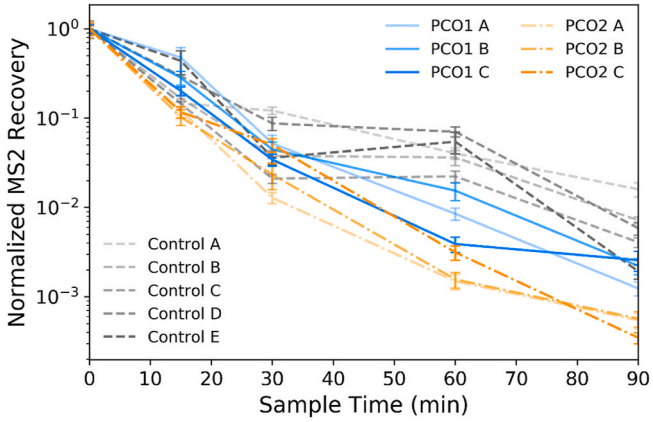

Fig. 5. Normalized MS2 recoveries at each sampling time point throughout the control and the two types of photocatalytic tests (PCO1 and PCO2) with the devices active. Each time point represents recovery of MS2 from duplicate bioaerosol samples as determined by plaque assay, and the error bars represent pooled standard deviation from triplicate sample plating of duplicate bioaerosol samples for each sampling time point. Data from each sampling time point are normalized to the initial sample recovery at time = 0 min for each individual test.

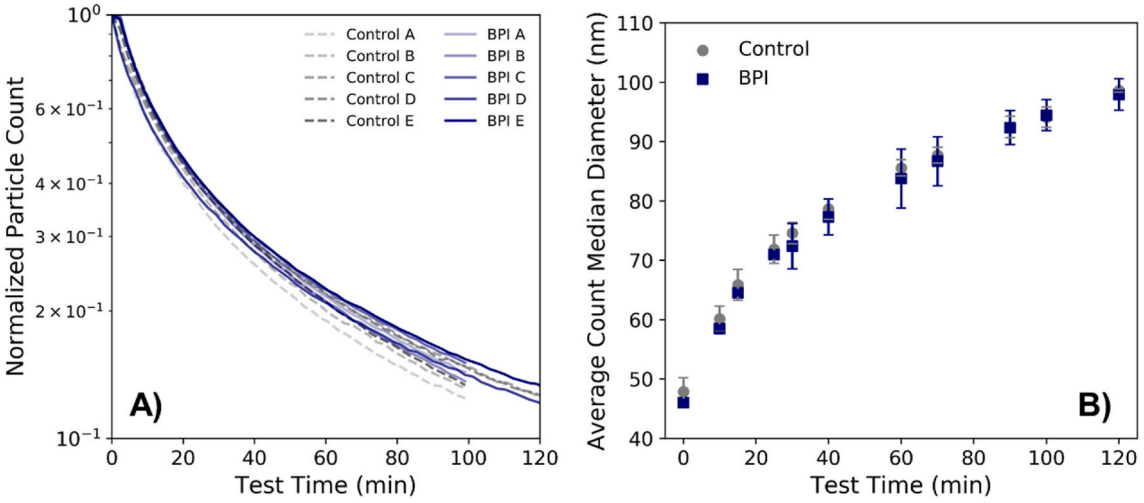

Fig. 4. A) Concentration of particles measured over the test period for both bipolar ionization (BPI) and control tests, normalized to the highest particle concentration measured during each respective test. B) Count median diameter as measured over the test period, averaged over each set of control and BPI tests, where error bars represent standard deviation among each type of experiment.

of 9.7 × 10^7 PFU/m^3 (average initial concentration of 8.3 ± 0.3 $\log_{10}$ PFU/m^3, averaged across photocatalytic tests and controls). The variability between normalized MS2 recoveries from the same sampling time point during test replicates ranges up to nearly 0.6 $\log_{10}$ for both the PCO1 and PCO2 units (at 60 and 30 min, respectively).

The average concentrations for each replicate set of photocatalytic and control tests, as well as the calculated $\log_{10}$ reductions at each sampling time point, are shown in Fig. 6, and the calculated $\log_{10}$ reductions are also listed in Table 1. As with the bipolar ionization device tests, the highest $\log_{10}$ reduction values occur at time = 60 min, with an approximate reduction in recovered MS2 of 1.1 $\log_{10}$ (91% reduction) for the PCO1 unit and 1.8 $\log_{10}$ (98% reduction) for the PCO2 unit. Following a normality check (Table S1), Welch's *t*-test was used to compare the normalized MS2 recoveries from the PCO1 and PCO2 tests to the control recoveries, and statistically significant differences (at the $\alpha = 0.05$ level) between the control and technology tests are observed at both the 60- and 90-min sampling time points for both of the photocatalytic devices (Table 1). The CADRs for the photocatalytic devices calculated for MS2 based on these results are 68 ft^3/min and 125 ft^3/min for the PCO1 and PCO2 devices, respectively (Fig. S3).

The total particle concentration in the test chamber over time during each experiment (where particle counts are again normalized to the maximum count during each test, which generally corresponds to the initial measurement) is shown in Fig. 7A. Similar to the bipolar ionization device tests, the particle concentrations during the photocatalytic device tests fell within the range of particle counts from the control tests. The average CMD particle size over the course of testing is shown in Fig. 7B; the sizes were generally similar between the photocatalytic and control experiments over time, although the average CMD was slightly larger for the PCO2 tests, most noticeably during the second half of the experiments.

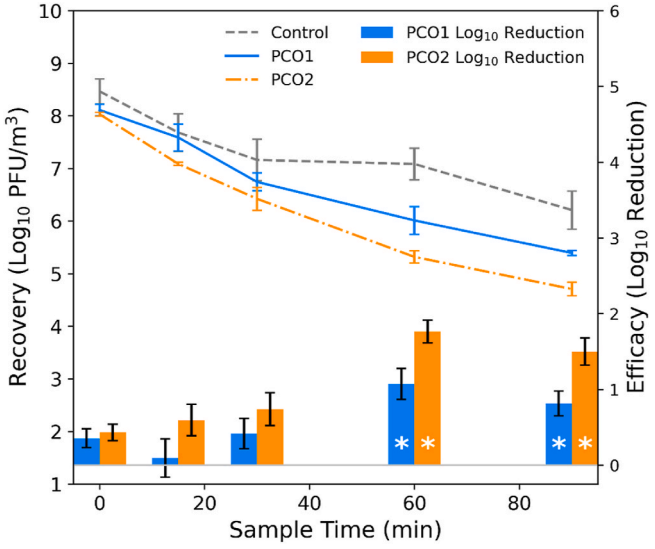

Fig. 6. (Left axis) Concentration of MS2 in the air at each sampling time point during the control and photocatalytic (PCO1 and PCO2) test experiments, averaged over each type of test, where error bars represent standard deviation from each set of recoveries. (Right axis) Efficacy of the PCO1 and PCO2 devices against aerosolized MS2, calculated as $\log_{10}$ reduction in MS2 recoveries from the control vs. photocatalytic test experiments; statistical significance between control and technology experiments at the sample times is denoted by (*). For recoveries, error bars represent standard deviation in $\log_{10}$ recoveries for each respective set of control and BPI experiments at each sample time; for efficacy, the error bars represent pooled standard error from both the control and technology experiments.

3.3. Deposition coupons

Deposition coupons (blank pieces of stainless-steel material, see Section 1.2.4, MS2 Surface Samples) were included in control tests A, B, C, and E; BPI tests A, B, and D; and PCO1 test C. After each test, MS2 was recovered from the deposition coupons, meaning that infectious virus was settling out of the air and onto surfaces during testing. The MS2 recovery (in $\log_{10}$ PFU/m^2) averaged over each test type is shown in Fig. 8. Following a normality check (Table S3), a *t*-test was used to compare MS2 recoveries from the replicate control and BPI tests (Table S4); no statistically significant differences were observed between recoveries from the control and technology tests at each of the deposition coupon locations. Similarly, a *t*-test comparing deposition coupon recoveries between the control and BPI tests, pooled over all locations, showed no statistical difference between recoveries from the full set of deposition coupons included in the control tests compared to that of the BPI tests (Table S4, all p-values > 0.2). An additional *t*-test comparing the recoveries (pooled over all locations) from the control tests and those from the PCO1 test showed no statistical difference between the two sets of coupons (Table S4).

3.4. Inactivation coupons

Inactivation coupons (small pieces of stainless-steel material inoculated with MS2, see Section 1.2.4, MS2 Surface Samples) were included in control tests C and E, BPI test D, and PCO1 test C. For each test, a set of positive controls (coupons inoculated and extracted following the same procedure as the inactivation coupons but kept outside the test chamber during testing) was also included. Fig. 9 shows the MS2 recoveries averaged over each test and coupon type. The calculated $\log_{10}$ reduction (subtracting average MS2 recoveries of the chamber coupons from the positive controls) is 0.39 $\log_{10}$ for the control tests, while those for the BPI and PCO1 tests were lower (0.36, and 0.17 $\log_{10}$, respectively).

4. Discussion

The antimicrobial efficacy of the technologies over time can be assessed by comparing the average concentration of MS2 recovered from the air throughout testing with each technology active compared to time-matched control tests (conducted under the same conditions, except without the technologies active). The only statistically significant difference between the average MS2 recoveries from the control and bipolar ionization tests occurs at the time = 60 min sampling time point, where the calculated $\log_{10}$ reduction was 0.88 (87%). Statistically significant differences were observed between tests with both photocatalytic devices and the control tests at 60 and 90 min, with the highest calculated $\log_{10}$ reductions for both technologies occurring at the 60 min sampling time point ($\log_{10}$ reductions of 1.1 [91%] and 1.8 [98%] for the PCO1 and PCO2 units, respectively). The average MS2 concentration from the control tests at the 60 min sampling time point was elevated above the general trend of sample recoveries from the other time points, which contributed to the largest calculated efficacies at this period during the testing (Figs. 2 and 5). The efficacy of both technologies during testing was greater at 60 min and beyond during the testing period, compared to the earlier time points during testing. This could be a result of the ratio between inactivation mechanism (e.g., ions, ozone) and the bacteriophage concentration becoming sufficiently high at this period during testing for the treatment technology to become more significantly effective, whether the increase in that ratio is a result of a growing concentration of the inactivation mechanism (e.g., increasing ion or ozone concentration over time), or a decreasing concentration of virus in the air (as a result of particle settling and natural decay), or some combination of the two.

Calculating the CADR for each set of technology tests is also insightful in evaluating antimicrobial efficacy of the devices, and it is particularly useful for extrapolating device performance in laboratory

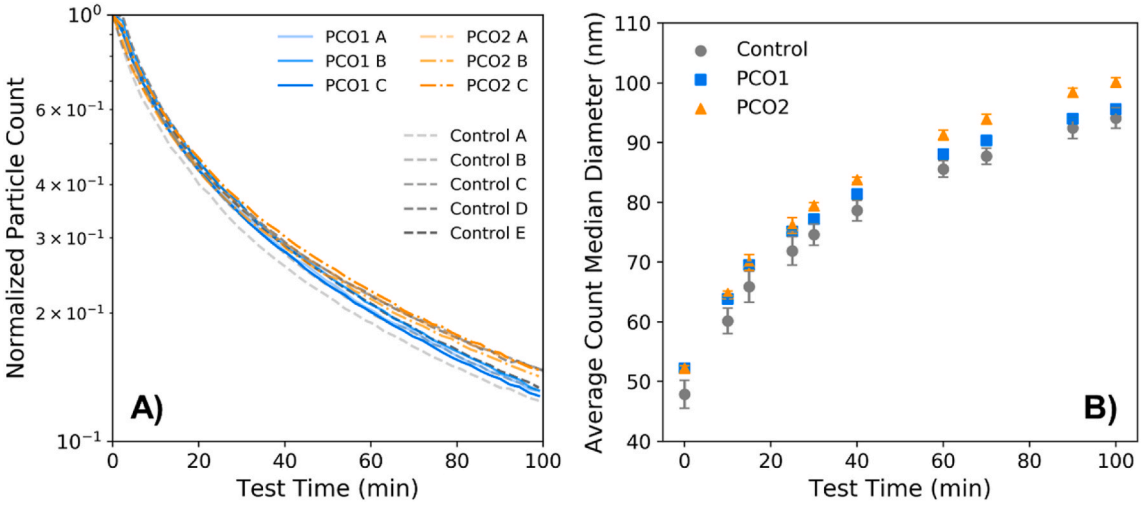

Fig. 7. A) Concentration of particles measured over the test period for both photocatalytic device tests (PCO1 and PCO2) and the control tests, normalized to the highest particle concentration measured during each respective test. B) Count median diameter as measured over the test period, averaged over each test type, where error bars represent standard deviation among each type of experiment.

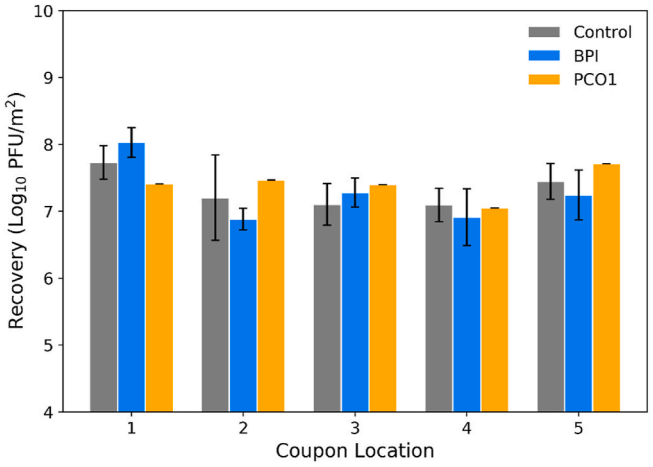

Fig. 8. The amount of viable MS2 deposited on surfaces during control, bipolar ionization (BPI), and photocatalytic device (PCO1) experiments, represented by the concentration of MS2 recovered from stainless-steel coupons initially inserted into the test chamber blank, averaged over each test type and coupon location (error bars represent standard deviation).

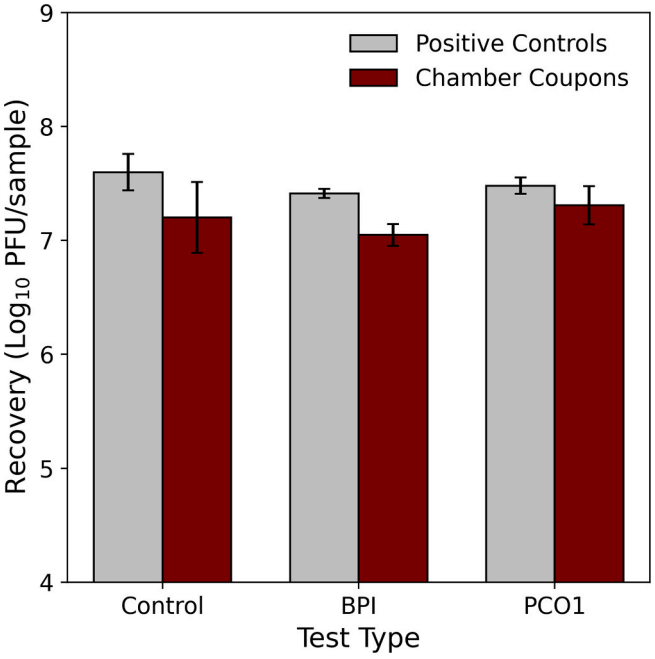

Fig. 9. The amount of MS2 recovered from stainless-steel coupons that were inoculated with MS2 prior to control, bipolar ionization (BPI), and photocatalytic (PCO1) experiments, where the chamber coupons were placed on the chamber floor throughout the duration of testing, and the positive controls, which were held outside of the chamber but otherwise treated in the same manner as the chamber coupons. Recoveries are averaged over each test type and all of the coupon locations in the chamber, and error bars represent standard deviation in recoveries.

tests to applied settings [42]. Generally, AHAM typically recommends that the CADR should be, at a minimum, 2/3 of the square footage of a room where it is deployed. Based on the results presented here, the minimum appropriate room sizes for the devices evaluated here would be approximately 51 ft^2 for the BPI, and 102 ft^2 for the PCO1, and 188 ft^2 for the PCO2 devices. Defining a singular ideal CADR for airborne pathogens is impossible based on the complexity of airborne disease transmission (i.e., the infectious dose varies depending on the microorganism, among many other factors), but of note is that the suitable room footprints based on the general AHAM CADR recommendations are small compared to many of the intended use cases for these devices (and they do not take harmful emission or by-product formation into account).

The concentration of viable MS2 in the air declined up to >3 log_{10} in the control tests over the course of 2 h. This decline, which is not attributable to any treatment technology (because none were active during the control tests), occurs because of natural decay, wall loss, and settling of MS2 over the test period. To properly evaluate efficacy of treatment technologies, it is critical to compare testing conducted with the treatment technologies to time-matched control tests, which account for these declining concentrations in the absence of treatment. Calculating efficacy based on log_{10} reductions compared to the initial bioaerosol concentration will overstate efficacy.

The observed variability in MS2 recoveries at the same sampling time points ranged up to nearly 1 log_{10} for the control tests and slightly greater than that for the technology tests (1.2 log_{10}). This variability, which arises even with the same test conditions, is inherent in conducting biological testing (in particular, bioaerosol testing [43]) and

underscores the importance of conducting replicate testing. This is particularly the case in evaluating the efficacy of technologies where there is notable overlap in measured recoveries from control and technology test conditions during the test period; for example, for the bipolar ionization device tests, there is overlap between the range of normalized MS2 recoveries between the control and technology tests at every single sampling time point. Moreover, the range of recoveries at some sampling time points from each respective set of control and bipolar ionization tests is greater than the overall largest calculated $\log_{10}$ reduction for the bipolar ionization device. Calculating efficacy based on any single control experiment compared to any single technology experiment would lead to a wide range of calculated efficacies (in both the positive and negative directions) as a result of the inherent testing variability. Therefore, calculating log reductions based on the mean recoveries from replicate testing (here, a minimum of three replicates for each test and control condition), is critical for meaningful efficacy evaluations of these air treatment technologies.

There was appreciably less variability in the particle measurements compared to the bioaerosol recoveries. For all tests, particle number concentration declined over time as a result of particle agglomeration, wall loss, and settling. The particle concentration and CMD were similar for the control and bipolar ionization experiments, suggesting that the bipolar ionization device does not appreciably impact particle dynamics under these test conditions. For the photocatalytic devices, the particle concentrations and CMDs were also fairly consistent among the control and both sets of technology tests, although the particle concentrations and CMDs were observably higher for the larger 9-inch photocatalytic cell (PCO2) compared to the smaller cell (PCO1, Fig. 7), suggesting that the larger unit may impact particle dynamics under these test conditions, potentially either from particles interacting with the technology emissions or its byproducts (although further investigation of these differences were beyond the scope of this study).

The amount of MS2 recovered from the surface of the initially clean deposition coupons was not statistically different between the control and technology tests, suggesting that neither technology impacted the rate at which viable MS2 was settling and deposited on surfaces in the chamber under these test conditions. For the inoculated coupons (inactivation coupons), the average difference between the positive controls (not exposed to the technology in the chamber) and the coupons deployed in the chamber was greatest for the control test (compared to the difference from the technology tests), meaning that the technologies deployed in the HVAC system did not demonstrate any additional efficacy against MS2 on surfaces under the conditions tested here.

This study evaluated the efficacy of two different technologies that have been designed to inactivate airborne pathogens at a scale that is translatable real-world conditions. However, as with any laboratory study, there are important limitations to recognize and consider when extrapolating these findings to applied settings. These tests were designed to create a high viral load in the chamber air that would persist over time, such that the concentration of bioaerosols in the chamber during control tests was high enough for any technology to be able to demonstrate a 3-$\log_{10}$ dynamic range in efficacy testing. As such, the viral load in the chamber air was relatively high, and the viral aerosol particle sizes were relatively small [43,44], so that a sufficiently high number of particles remained lofted in the chamber throughout the duration of testing. Many other factors, including humidity, temperature, and suspension medium, impact the survivability and resistance of airborne microorganisms to inactivation mechanisms [45–47]. In this study, 100% of the air was recirculated, and no fresh air was introduced into the chamber during testing; in applied settings, air dilution (either through direct introduction of fresh "makeup" air into the HVAC system, or, for example, from the opening/closing of doors on a transit vehicle) will reduce concentrations of airborne pathogens; however, it will also reduce concentrations of technologies that rely on a sufficient amount of the inactivation mechanism per volume in the air to be effective (e.g., chemical, ions, etc.). The bacteriophage release in these experiments was not representative of more continuous and persistent viral shedding processes, which may be more representative of some real-world settings (compared to an initial high concentration injection), but viral shedding processes are known to be highly dynamic, variable, and impacted by many factors [48,49]. Those considerations aside, the research presented here demonstrates that standardized testing of air treatment technologies against airborne microorganisms (and microorganisms on surfaces) at scales that are representative of applied settings can provide an effective and comparable way to evaluate the potential efficacy of these air treatment technologies.

As air cleaning devices have become more widely available, marketed, and installed in indoor settings, there has also been a growing concern about the potential unintended health effects from chronic exposure to even low levels of primary and secondary products generated by these technologies. Air ionization and photocatalytic oxidation devices generate reactive species, including ozone, which can in turn form byproducts including semivolatile and volatile organic compounds, generate particulate matter, and degrade indoor materials [50]. Exposure to high ion levels has also been associated with negative health effects and oxidative stress [51]. The photocatalytic devices evaluated in this study produced elevated levels of ozone in the test chamber (average concentration of 105 ppb and 131 ppb at 60 and 90 min, respectively). For reference, the OSHA 8-h time-weighted average permissible exposure limit (PEL-TWA) is 100 ppb. Additional research is needed to more fully characterize exposure levels and understand the potential health impacts from prolonged exposure to products and byproducts generated by air cleaning technologies [33].

5. Conclusions

This study demonstrates that a large-scale test chamber with a recirculating HVAC system and a standardized testing approach can be used to evaluate the efficacy of air treatment devices against MS2 in the air and on surfaces. Conducting experiments in this way generates results that are more readily extrapolated to applied settings and facilitates comparison across different technology types. Because natural decay, wall loss, and settling of MS2 in the control tests can account for up to a 3 $\log_{10}$ reduction in bioaerosol concentrations over 2 h, performing time-matched control tests is necessary for evaluating efficacy that is attributable to the technologies themselves. Moreover, because the variability in average MS2 recoveries can vary >1 $\log_{10}$ at each sampling time point in a particular set of experiments, conducting replicate experiments is also essential. The bipolar ionization and photocatalytic devices were more effective later in the test period, with a peak $\log_{10}$ reduction of 0.88 for the bipolar ionization device and 1.8 $\log_{10}$ reduction for the larger photocatalytic device, occurring for both types of technologies at 60 min. None of the technologies tested appreciably impacted particle concentrations, size distributions, or deposition rates, nor did they demonstrate efficacy against MS2 on surfaces in the test chamber. Although the bipolar ionization device, which contains an ozone catalyst, did not raise ozone concentrations above background levels, the larger photocatalytic device, which demonstrated the highest efficacy, exceeded the OSHA PEL, underscoring the need to evaluate and monitor primary or secondary emissions when considering potential deployment of air treatment technologies that emit reactive species.

Disclaimer

The EPA, through its Office of Research and Development, directed the research described herein conducted through contract 68HERC20D0018 with Jacobs Technology, Inc. It has been subjected to the Agency's review and has been approved for publication. Mention of trade names, products or services does not convey official EPA approval, endorsement, or recommendation.

CRediT authorship contribution statement

Katherine M. Ratliff: Writing – original draft, Visualization, Supervision, Project administration, Methodology, Formal analysis, Data curation, Conceptualization. **Lukas Oudejans:** Writing – review & editing, Supervision, Methodology, Conceptualization. **John Archer:** Writing – review & editing, Methodology, Conceptualization. **Worth Calfee:** Writing – review & editing, Methodology, Conceptualization. **Jerome U. Gilberry:** Writing – review & editing, Project administration, Methodology, Investigation, Conceptualization. **David Adam Hook:** Project administration, Methodology, Investigation, Formal analysis, Data curation. **William E. Schoppman:** Writing – review & editing, Methodology, Investigation, Data curation. **Robert W. Yaga:** Writing – review & editing, Methodology, Investigation, Formal analysis, Data curation. **Lance Brooks:** Writing – review & editing, Methodology, Conceptualization. **Shawn Ryan:** Writing – review & editing, Methodology, Conceptualization.

Declaration of competing interest

The authors declare that they have no known competing financial interests or personal relationships that could have appeared to influence the work reported in this paper.

Data availability

All data supporting this study and manuscript are available on data.gov.

Acknowledgements

The authors gratefully acknowledge the members of the EPA Project Team, the members of Jacobs Technology, Inc. (JTI) supporting the EPA Homeland Security and Materials Management Microbiology Lab and JTI Aerosol Science Team, Anne Mikelonis and Jillianne Taylor for internal technical reviews of this manuscript, Ramona Sherman for quality assurance support, and two anonymous peer reviewers for constructive feedback that improved the quality of this manuscript.

Appendix A. Supplementary data

Supplementary data to this article can be found online at https://doi.org/10.1016/j.buildenv.2022.109804.

References

[1] L. Bourouiba, The fluid dynamics of disease transmission, Annu. Rev. Fluid Mech. 53 (1) (2021) 473–508.
[2] C.F. Dillon, M.B. Dillon, Multiscale Airborne infectious disease transmission, Appl. Environ. Microbiol. 87 (4) (2021) e02314–e02320.
[3] National Academies of Sciences, Engineering, and Medicine, The National Academies collection: reports funded by National institutes of health, in: A. Staudt, et al. (Eds.), Airborne Transmission of SARS-CoV-2: Proceedings of a Workshop—In Brief, National Academies Press (US), Washington (DC), 2020.
[4] Z. Peng, et al., Practical indicators for risk of airborne transmission in shared indoor environments and their application to COVID-19 outbreaks, Environ. Sci. Technol. 56 (2) (2022) 1125–1137.
[5] K.A. Prather, et al., Airborne transmission of SARS-CoV-2, Science 370 (6514) (2020) 303–304.
[6] J.M. Samet, et al., Airborne transmission of severe acute respiratory syndrome coronavirus 2 (SARS-CoV-2): what we know, Clin. Infect. Dis. 73 (10) (2021) 1924–1926.
[7] J.W. Tang, et al., Dismantling myths on the airborne transmission of severe acute respiratory syndrome coronavirus-2 (SARS-CoV-2), J. Hosp. Infect. 110 (2021) 89–96.
[8] C.C. Wang, et al., Airborne transmission of respiratory viruses, Science 373 (6558) (2021) eabd9149.
[9] A. Katelaris, et al., Epidemiologic evidence for airborne transmission of SARS-CoV-2 during Church singing, Australia, 2020, Emerg. Infect. Dis. 27 (6) (2021) 1677.
[10] Y. Li, et al., Probable Airborne Transmission of SARS-CoV-2 in a Poorly Ventilated Restaurant, Building and Environment, 2021, 107788.
[11] Y. Shen, et al., Community outbreak investigation of SARS-CoV-2 transmission among bus riders in Eastern China, JAMA Intern. Med. 180 (12) (2020) 1665–1671.
[12] L. Morawska, et al., How can airborne transmission of COVID-19 indoors be minimised? Environ. Int. 142 (2020), 105832.
[13] E. Eadie, et al., Far-UVC (222 nm) efficiently inactivates an airborne pathogen in a room-sized chamber, Sci. Rep. 12 (1) (2022) 4373.
[14] T.T. Nguyen, et al., A systematic literature review of indoor air disinfection techniques for airborne bacterial respiratory pathogens, Int. J. Environ. Res. Publ. Health 19 (3) (2022) 1197.
[15] U.S. EPA, Residential Air Cleaners - A Technical Summary, 2018.
[16] Y. Zeng, M. Heidarinejad, B. Stephens, Evaluation of an in-duct bipolar ionization device on particulate matter and gas-phase constituents in a large test chamber, Build. Environ. 213 (2022), 108858.
[17] A. Bisag, et al., Cold atmospheric plasma inactivation of aerosolized microdroplets containing bacteria and purified SARS-CoV-2 RNA to contrast airborne indoor transmission, Plasma Process. Polym. 17 (10) (2020), 2000154.
[18] S.-G. Lee, et al., One-pass antibacterial efficacy of bipolar air ions against aerosolized Staphylococcus epidermidis in a duct flow, J. Aerosol Sci. 69 (2014) 71–81.
[19] S.S. Nunayon, et al., Experimental evaluation of positive and negative air ions disinfection efficacy under different ventilation duct conditions, Build. Environ. 158 (2019) 295–301.
[20] H. Qin, et al., Efficient disinfection of SARS-CoV-2-like coronavirus, pseudotyped SARS-CoV-2 and other coronaviruses using cold plasma induces spike protein damage, J. Hazard Mater. 430 (2022), 128414.
[21] N.D. Vaze, et al., Involvement of multiple stressors induced by non-thermal plasma-charged aerosols during inactivation of airborne bacteria, PLoS One 12 (2) (2017) e0171434.
[22] J.H. Park, K.Y. Yoon, J. Hwang, Removal of submicron particles using a carbon fiber ionizer-assisted medium air filter in a heating, ventilation, and air-conditioning (HVAC) system, Build. Environ. 46 (8) (2011) 1699–1708.
[23] B. Shi, L. Ekberg, Ionizer assisted air filtration for collection of submicron and ultrafine particles—evaluation of long-term performance and influencing factors, Environ. Sci. Technol. 49 (11) (2015) 6891–6898.
[24] M. Baselga, J.J. Alba, A.J. Schuhmacher, Impact of needle-point bipolar ionization system in the reduction of bioaerosols in collective transport, Sci. Total Environ. 855 (2022), 158965, https://doi.org/10.1016/j.scitotenv.2022.158965.
[25] Y.-Y. Wu, et al., Deposition removal of monodisperse and polydisperse submicron particles by a negative air ionizer, Aerosol Air Qual. Res. 15 (3) (2015) 994–1007.
[26] M. Pelaez, et al., A review on the visible light active titanium dioxide photocatalysts for environmental applications, Appl. Catal. B Environ. 125 (2012) 331–349.
[27] J.A. Byrne, et al., A review of heterogeneous photocatalysis for water and surface disinfection, Molecules 20 (4) (2015) 5574–5615.
[28] A. Habibi-Yangjeh, et al., Review on heterogeneous photocatalytic disinfection of waterborne, airborne, and foodborne viruses: can we win against pathogenic viruses? J. Colloid Interface Sci. 580 (2020) 503–514.
[29] N. Bono, et al., Effect of UV irradiation and TiO2-photocatalysis on airborne bacteria and viruses: an overview, Materials 14 (5) (2021) 1075.
[30] H. Destaillats, et al., Key parameters influencing the performance of photocatalytic oxidation (PCO) air purification under realistic indoor conditions, Appl. Catal. B Environ. 128 (2012) 159–170.
[31] U.S. EPA, OCSPP 810.2200: Disinfectants for Use on Environmental Surfaces, Guidance for Efficacy Testing, U.S. Environmental Protection Agency, 2018.
[32] Association of Home Appliance Manufacturers, AC-5-2022, Method for Assessing the Reduction Rate of Key Bioaerosols by Portable Air Cleaners Using an Aerobiology Test Chamber, 2022. Washington DC.
[33] National Academies of Sciences, Engineering, and Medicine, Why Indoor Chemistry Matters, 2022. Washington, DC.
[34] E.H. Spaulding, E.K. Emmons, Chemical disinfection, Am. J. Nurs. 58 (9) (1958) 1238–1242.
[35] ANSI/ASHRAE, *Standard 62.1-2019, Ventilation for Acceptable Indoor Air Quality*, American Society of Heating, Refrigerating, and Air-Conditioning Engineers, Atlanta, GA, 2019.
[36] ANSI/ASHRAE, *Standard 62.2-2019, Ventilation and Acceptable Indoor Air Quality in Residential Buildings*, American Society of Heating, Refrigerating, and Air-Conditioning Engineers, Atlanta, GA, 2019.
[37] U.S. EPA, Product Performance Test Guidelines: OCSPP 810.2500: Air Sanitizers - Efficacy Data Recommendations, 2012.
[38] K. Lin, L.C. Marr, Humidity-dependent decay of viruses, but not bacteria, in aerosols and droplets follows disinfection kinetics, Environ. Sci. Technol. 54 (2) (2020) 1024–1032.
[39] W.A. Rutala, D.J. Weber, Selection of the ideal disinfectant, Infect. Control Hosp. Epidemiol. 35 (7) (2014) 855–865.
[40] A.M. Kropinski, et al., Enumeration of bacteriophages by double agar overlay plaque assay, in: M.R.J. Clokie, A.M. Kropinski (Eds.), Bacteriophages: Methods and Protocols, Volume 1: Isolation, Characterization, and Interactions, Humana Press, Totowa, NJ, 2009, pp. 69–76.
[41] A.M. Kropinski, et al., Enumeration of bacteriophages by double agar overlay plaque assay, in: Bacteriophages, Springer, 2009, pp. 69–76.
[42] B. Stephens, et al., Interpreting Air Cleaner Performance Data 64 (3) (2022) 20–30.
[43] M. Alsved, et al., Natural sources and experimental generation of bioaerosols: challenges and perspectives, Aerosol. Sci. Technol. 54 (5) (2020) 547–571.
[44] M. Dybwad, G. Skogan, Aerobiological stabilities of different species of gram-negative bacteria, including well-known biothreat simulants, in single-cell particles

and cell clusters of different compositions, Appl. Environ. Microbiol. 83 (18) (2017) e00823-17.
[45] A.E. Haddrell, R.J. Thomas, D.W. Schaffner, Aerobiology: experimental considerations, observations, and future tools, Appl. Environ. Microbiol. 83 (17) (2017) e00809–e00817.
[46] E. Huynh, et al., Evidence for a semisolid phase state of aerosols and droplets relevant to the airborne and surface survival of pathogens, Proc. Natl. Acad. Sci. USA 119 (4) (2022) e2109750119.
[47] Z. Zuo, et al., Survival of airborne MS2 bacteriophage generated from human saliva, artificial saliva, and cell culture medium, Appl. Environ. Microbiol. 80 (9) (2014) 2796–2803.
[48] N.H.L. Leung, et al., Respiratory virus shedding in exhaled breath and efficacy of face masks, Nat. Med. 26 (5) (2020) 676–680.
[49] J. Yan, et al., Infectious virus in exhaled breath of symptomatic seasonal influenza cases from a college community, Proc. Natl. Acad. Sci. USA 115 (5) (2018) 1081–1086.
[50] D.B. Collins, D.K. Farmer, Unintended consequences of air cleaning chemistry, Environ. Sci. Technol. 55 (18) (2021) 12172–12179.
[51] W. Liu, et al., Negative ions offset cardiorespiratory benefits of PM2.5 reduction from residential use of negative ion air purifiers, Indoor Air 31 (1) (2021) 220–228.